Delamination of an orthotropic cylindrical shell with helically wound fiber reinforcement when subjected to Axial Compression

Afroz Mehar[#1], P. Ravinder Reddy[#2], G.K. Mohan Rao[#3], S.Irfan Sadaq[#4]

[#] *Assistant Professor, Mechanical Engineering Dept, M.J.C.E.T, Hyderabad, India.*

[1]afrozmehar786@gmail.com

[4]irfan.ajai@gmail.com

[2]*Prof & Head, Mechanical Engineering Dept, C.B.I.T, Hyderabad, India.*

[3]*Associate Professor*, Mechanical Engineering Dept *JNTU, Hyderabad*, India.

Abstract The delamination growth may occur in delaminated cylindrical shells under Axial Buckling. This will lead to failure of structure. This paper deals with the instability analysis of delaminated composite cylindrical shells subject to axial compression, using the finite element method. The effect of contact in the buckling mode has been considered, by employing contact elements between the delaminated layers. The interactive buckling curves response of delaminated cylindrical shells has been obtained. It was also observed that the effects of delamination are more apparent when the composite cylindrical shells are subjected to combined axial compression and bending. Using finite element analysis (Ansys) we have found different mode shapes reacting with respect to the winding angle affecting the properties of the cylindrical shell.
Key words: composite, laminated cylindrical shell, delamination growth, energy release rates, contact effect

I.   INTRODUCTION

Composite laminates are widely used in engineering because of their specific excellent properties, such as high strength-to-weight ratio, high stiffness-to-weight ratio, designability, and so forth. But there will be delamination damage in composite laminates during the manufacturing processes, for instance, shocks in assembling procedures. When compared with axial pressure, external pressure does not cause local buckling in delaminated composite laminates, but it can drive in the growth of the delamination. And this will drastically reduce the stiffness and the carrying capacity of the laminated structure, resulting in global buckling and failure of structure at last. It is necessary to determine the stress fields of delamination front in order to analyze the delamination growth of laminated structures. Laminated composite materials are increasingly being used in the aerospace, marine, automobile and other engineering industries. This is due to their high strength-to weight and stiffness-to-weight ratios. However, due to the lack of through-the-thickness reinforcement, structures made from these materials are highly liable to failures caused by delamination. Therefore, within a design process, a structure's resistance to delamination should be addressed to maximize its durability and damage tolerance. Delaminations in composite cylinders may be due to manufacturing defects, transportation impacts and environmental effects during their service life. The presence of delaminations leads to a reduction in the overall buckling strength of the laminated composite cylindrical shells [3–6]. For the past two decades analytical and numerical analyses have been carried out by many researchers to analyze delaminated composite structures, considering their buckling and post-buckling behaviour [7,8]. Almost all of the papers on delamination buckling deal with beams and flat plates. [6,9–17]. The early work belongs to Chai et al. [9] who characterized the delamination buckling models by the delamination thickness and the number of delaminations through the laminate thickness. Due to its mathematical complexity and modelling, very limited information on the subject of delamination buckling of cylindrical shells and panels is currently available [3–5,18–28]. .

This paper deals with the computational modelling of delamination buckling of filament wound composite cylindrical shells subjected to axial compression using Ansys.

II.   GEOMETRY, MATERIALS AND LOADING CONDITIONS
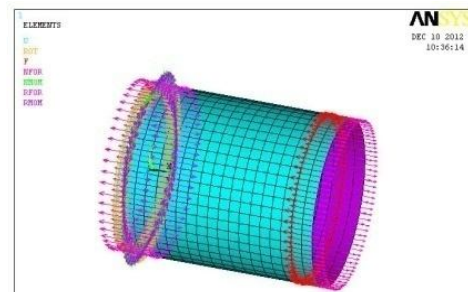
Fig. 1. Cylindrical shell with different loading conditions

A typical delaminated circular cylindrical shell with length L=18cm, radius r=7.6, and thickness t=0.152cm is shown in Fig. 1. The axial coordinate is x, the circumferential coordinate is y, and the through-the-thickness coordinate normal to the shell middle surface is z. The circumferential

coordinate is replaced by y = rβ. The rectangular delamination (L_d x b) is located symmetrically with respect to both ends of the shell, where L_d is in the axial direction and b = rα is in the circumferential direction. Angle α denotes the region of the delamination.t_1 and t_2 are the thicknesses of the upper and lower sublaminantes, respectively. The loadings considered in this study are axial compressive load. The axial load (R) is a uniform compressive applied at the ends of the shell. In this study the delamination surface is always symmetric with respect to the plane . The materials selected throughout this study and their engineering constants are shown in Table 1. Fig. 1c–e show the first buckling mode of a glass/epoxy cylindrical shell (L/r =2.4,r/t =50) with the stacking sequence of [0/0/0], [30/30/30], [45/45/45], [60/60/60] [90/90/90] under axial compression.

III. FINITE ELEMENT MODELING

The following explains the FE modelling, buckling procedures and also the method employed for calculation of the strain energy release rate (SERR) in this study, respectively. The displacement field for an intact cylindrical shell, according to a first order shear deformation theory, is given by

$$u_x = u_x^0 + z\psi_x$$
$$u_y = u_y^0 + z\psi_y$$
$$u_z = u_z^0$$

--------------(1)

ux, uy, uz are the displacements (in the x, y and z directions, respectively) and ψ_x, ψ_y are the rotations (about y and x axes, respectively), at arbitrary locations with the distance z to the shell's mid-surface. u_x^0, u_v^0, u_z^0 are the mid-surface displacements of the shell in the respective directions. For the analysis of a delaminated cylinder, the intact regions can be represented by a single-layer of shell elements, whereas the delaminated regions can be modelled by upper and lower sublaminates that are connected by contact elements.
For the interface region, a modified version of the sublaminate connection method, based on Eq. (1), must be employed. Therefore, also the rotations (ψ_x, ψ_y, ψ_z) of all the nodes of the stacked layers at the transition border are coupled in addition to the displacements (u_x, u_v, u_z). Thus, the mid-surfaces of the sublaminates of the delaminated and the mid-surface of the laminate of the intact area are coupled by the following set of equations:

$$u_x^{1,0} - \left(\frac{t_1}{2}\right)\psi_x^1 = u_x^{2,0} + \left(\frac{t_2}{2}\right)\psi_x^2 = u_x^0$$
$$u_y^{1,0} - \left(\frac{t_1}{2}\right)\psi_y^1 = u_y^{2,0} + \left(\frac{t_2}{2}\right)\psi_y^2 = u_y^0$$
$$u_z^{1,0} = u_z^{2,0} = u_z^0$$
$$\psi_x^1 = \psi_x^2 = \psi_x^0$$
$$\psi_y^1 = \psi_y^2 = \psi_y^0$$
$$\psi_z^1 = \psi_z^2 = \psi_z^0$$

-------------(2)

The selection of the mid-surface as a reference surface in a shell element is due to tradition and the ease of defining bending and shear rigidities. However, for composite laminates with delaminations, it leads to the complexity of using constraint equations (Eq. 2) to maintain compatibility of displacements on the delaminated front. The other disadvantage is for use with the virtual crack closure technique (VCCT) for calculation of the strain energy release rate (SERR). An alternative method, which overcomes these difficulties and also simplifies the mesh generation, is to choose the reference surface at an arbitrary position within the shell's thickness. According to the first order, shear deformation theory (Eq. 1), the deformation at any position within the thickness direction can be expressed by the deformation at any chosen surface, not necessarily the shell's mid-surface. Fig. 1 shows the close-up view of the FE model used in the present study. This FE model is also a combination of double-layer and single-layer of shell elements; however, the delaminated surface is chosen as the reference surface for both the intact and delaminated regions. In the delaminated region, nodes are separately defined on the upper and lower sublaminates although they may have the same coordinates. Within the intact and delaminated regions, the nodes located on the reference surface are offset from the mid-surfaces of the corresponding shells, either in the positive or negative direction. To maintain compatibility of displacements on the delaminated front, the nodes of the intact and delaminated regions are tied together to have equal deformations. The first stage in the simulation of the delaminated cylinder subject to axial compression is a linear eigen value buckling analysis. In simple cases, linear eigen value analysis may be sufficient for design evaluation; but geometrically nonlinear static problems sometimes involve buckling or collapse behaviour, where the load–displacement response shows a negative stiffness and the structure must release strain energy to remain in equilibrium. Several methods [33,34] are available for modelling such behaviour. It should be noted that the initial small deflection that is necessary to make the structure buckle was established by imposing an imperfection to the original mesh. The applied imperfection rested on an eigen mode buckling analysis of the structure where the maximum initial perturbation was 5% of the thickness of the shell. This method has been successfully

used in the earlier studies of the author [3,4,30]. For the buckling analysis, the axial compressive load is set to increase up to 1.2 times the critical axial compressive load of a perfect cylinder subjected to axial compressive load alone. Using Ansys it is also possible to apply an axial compressive load in the first step and to determine the critical bending moment in the following step. The results will be almost identical. The virtual crack closure technique (VCCT) is used to calculate the strain energy release rate (SERR). The nodal forces at the crack front and the displacements behind the crack front are used to calculate SERR [31]. The components of the strain energy release rate for the three modes for a typical element are

$$G_I = \frac{1}{2\Delta A} \left\{ F_{Z_{c_3}}(w_{a_3} - w_{A_3}) + F_{Z_{d_2}}(w_{b_2} - w_{B_2}) \right.$$
$$\left. + \frac{1}{2} \left[F_{Z_{c_2}}(w_{a_2} - w_{A_2}) + F_{Z_{c_4}}(w_{a_4} - w_{A_4}) \right] \right\}$$

$$G_{II} = \frac{1}{2\Delta A} \left\{ F_{X_{c_3}}(u_{a_3} - u_{A_3}) + F_{X_{d_2}}(u_{b_2} - u_{B_2}) \right.$$
$$\left. + \frac{1}{2} \left[F_{X_{c_2}}(u_{a_2} - u_{A_2}) + F_{X_{c_4}}(u_{a_4} - u_{A_4}) \right] \right\}$$

$$G_{III} = \frac{1}{2\Delta A} \left\{ F_{Y_{c_3}}(v_{a_3} - v_{A_3}) + F_{Y_{d_2}}(v_{b_2} - v_{B_2}) \right.$$
$$\left. + \frac{1}{2} \left[F_{Y_{c_2}}(v_{a_2} - v_{A_2}) + F_{Y_{c_4}}(v_{a_4} - v_{A_4}) \right] \right\} \quad \text{----------(3)}$$

An example of a delaminated cylindrical shell made of isotropic material with clamped ends under axial compression, similar to the model employed by Simitses et al. [20], was presented in Ref. [5] to validate the proposed FE modelling approach. The delamination was located symmetrically with respect to both ends of the shell and it extended along its entire circumference. The dimensions of the shell are such that L/r =2.4 and r/t = 50. The numerical results of variation of critical load with delamination length and delamination thickness, obtained using the present method, were compared with those obtained by Simitses et al. [20]. The critical loads (R_{cr}) are normalized with respect to the critical load of an intact cylinder (R_c). It is shown that although Simitses et al. [20] did not account for the contact, between delaminated layers during buckling, their results look reasonable. The cross-ply laminates had the stacking sequence of [0/0/0], [30/30/30], [45/45/45], [60/60/60] [90/90/90].
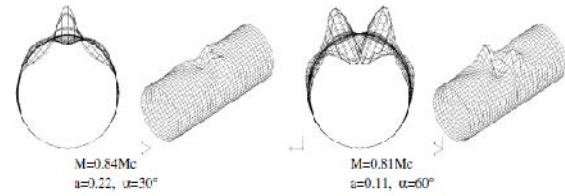
Fig. 2. The buckling behavior with different mode shapes

IV. RESULTS AND DISCUSSION

A cylindrical shell, with one end clamped, subjected to axial compression is presented here. The loading case of axial compression is considered. The dimensions of the shell employed throughout this study are such that L/r = 2.4 and r/t = 50. Throughout this study shell 99 element is chosen in ansys.
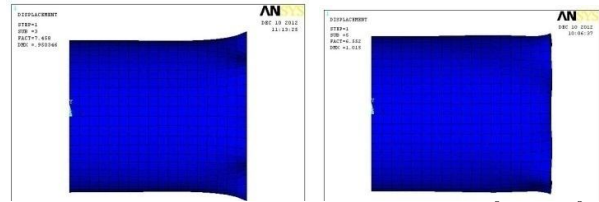
Fig. 3. Result for different mode shapes for 30^0 and 45^0 angles
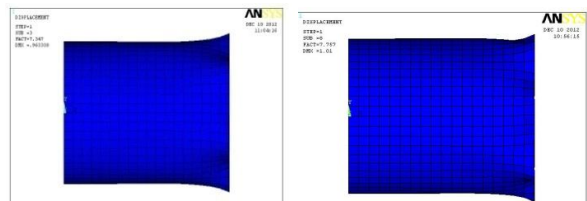
Fig . 4 Result for different mode shapes for 60^0 and 90^0 angles
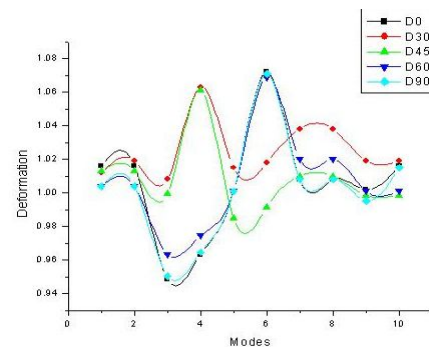
Fig.5 Deformation Vs mode shapes

ISSN 2278-3091

International Journal of Advanced Trends in Computer Science and Engineering, Vol.2 , No.1, Pages : 135-138 (2013)
Special Issue of ICACSE 2013 - Held on 7-8 January, 2013 in Lords Institute of Engineering and Technology, Hyderabad

The fig 5. Is the plot of deformation verses mode shape. It shows that the maximum deformation for the fiber angle 0, 60, 90 is acting at mode shape 6, where as in fiber angle30 and 45 it is acting at mode shape 4. Therefore the maximum deformation for the stacking sequence of glass/epoxy material is 1.072 .acting at mode 6.the deformation is less at mode shape between 2 and 4 so, this is the safest zone for the orthotropic cylindrical shell.
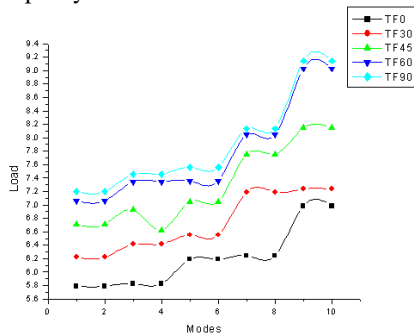
Fig. 6 Load Vs Mode shapes

The above figure shows that the maximum critical loads obtained are high for the 90 and 60 degree fiber angle. Almost for all the stacking sequence the loads are high at modes shapes 10. It means that to avoid failure this mode should be avoided

V. CONCLUSIONS

1. The critical buckling load is high for the stacking sequence of fiber angle at 90^0, therefore this angle is good to avoid critical buckling.
2. Deformation is less in fiber angle 0^0, 60^0, and 90^0. Therefore this can be used in combination to increase its buckling strength and improve the properties of helically wound cylindrical shells.
3. The helical angle of the cylindrical shell play an important role for its functionality.

REFERENCES

[1] Tafreshi A. Shape sensitivity analysis with respect to the positioning of features in composite structures using the boundary element method. Eng Anal Bound Elem 2006;30(1):1–13.
[2] Tafreshi A. Optimum shape design of composite structures using the boundary element method. AIAA J 2005;43(6):1349–59.
[3] Tafreshi A. Delamination buckling and postbuckling in composite cylindrical shells under combined axial compression and external pressure. J Compos Struct 2006;72(4):401–18.
[4] Tafreshi A. Delamination buckling and postbuckling in composite cylindrical shells under external pressure. Thin Wall Struct 2004;42/ 10:1379–404.

[5] Tafreshi A. Efficient modelling of delamination buckling in composite cylindrical shells under axial compression. Compos Struct 2004;64:511–20.
[6] Tafreshi A, Oswald T. Global buckling behaviour and local damage propagation in composite plates with embedded delaminations. Int J Press Ves Piping 2003;80(1):9–20.
[7] Bolotin VV. Delamination in composite structures: its origin, buckling, growth and stability. Composites: Part B 1996;27B: 129–45.
[8] Tay TE. Characterization and analysis of delamination fracture in composites: An overview of developments from 1990–2001. Appl Mech Rev 2003;56(1):1–31.
[9] Chai H, Babcock CA, Knauss WG. One dimensional modeling of failure in laminated plates by delamination buckling. Int J Solids Struct 1981;17(11):1069–83.
[10] Klug J, Wu XX, Sun CT. Efficient modelling of postbuckling delamination growth in composite laminates using plate elements. AIAA J 1996;34(1):178–84.
[11] Pavier MJ, Clarke MP. A specialised composite plate element for problems of delamination buckling and growth. Compos Struct 1996;34:43–53.
[12] Chattopadhyay A, Gu H. New higher order plate theory in modeling delamination buckling of composite laminates. AIAA J 1994;32(8):1709–16.
[13] Chai GB, Banks WM, Rhodes J. Experimental study on the buckling and postbuckling of carbon fibre composite panels with and without interply disbonds. Proceedings of the institution of mechanical engineers: design in composite materials. Mechanical Engineering Publications; 1989. p. 69–85.
[14] Whitcomb JD. Three-dimensional analysis of a postbuckled embedded delamination. J Compos Mater 1989;23(9):862–89.
[15] Hu N. Buckling analysis of delaminated laminates with consideration of contact in buckling mode. Int J Numer Meth Eng 1999;44: 1457–79.